

Promoting Effect of ZSM-5 Catalyst on Carbonization via Hydrothermal Conversion of Sewage Sludge

Chuan Peng,^{†,‡,§,||} Yunbo Zhai,^{*,†,‡,§,#} Andreas Hornung,^{||} Caiting Li,^{†,‡} Guangming Zeng,^{†,‡} and Yun Zhu^{*,§}

[†]College of Environmental Science and Engineering, Hunan University, Yuelu District, Changsha 410082, P. R. China

[‡]Key Laboratory of Environmental Biology and Pollution Control (Hunan University), Ministry of Education, Yuelu District, Changsha 410082, P. R. China

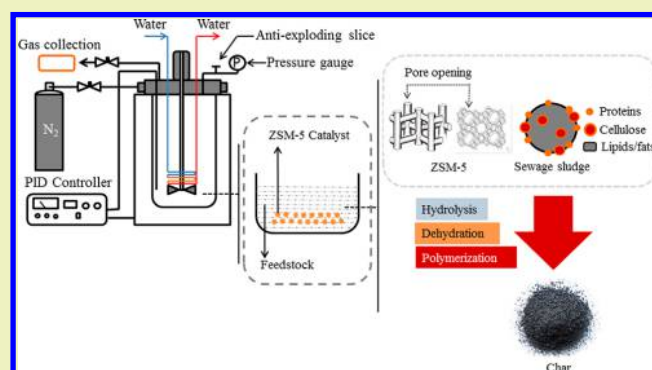
[§]Shenzhen Institutes of Hunan University, Nanshan District, Shenzhen 518000, P. R. China

^{||}Fraunhofer UMSICHT, Institute Branch Sulzbach-Rosenberg, An der Maxhütte 1, Sulzbach-Rosenberg 92237, Germany

[#]State Key Laboratory of Petroleum Pollution Control, Beijing 102206, China

ABSTRACT: An in-depth study on the transformation and distribution of carbons via hydrothermal conversion (HTC) of sewage sludge was conducted to evaluate the catalytic impact of Zeolite Socony Mobil-5 (ZSM-5). All the experiments were carried out between 180 and 300 °C with ZSM-5 catalyst during the HTC. Chars were analyzed for their carbon content distribution, carbonization degree, carbon-containing functional groups, and Raman chemical structural properties. The results revealed that ZSM-5 catalyst could concentrate carbon-containing matter in char and have distinct catalytic effects of ZSM-5 on carbonization degree. The catalyst with an Si/Al ratio of 300 is appropriate for char production at lower reaction temperatures, whereas the char with lower Si/Al ratio catalyst has better performance under higher reaction temperatures. ZSM-5 has a positive effect on the decomposition of C–(C,H) and promotes formation of C–(O,N) structure. Moreover, it can increase the decomposition of functional groups C≡N and enhance the formation of –CH_n groups. Compared to the pure char, the structure of char converted from a small aromatic ring to a larger aromatic ring with ZSM-5 catalyst assistant.

KEYWORDS: Sewage sludge, Char, Catalyst, Hydrothermal conversion, Carbon-containing compounds



INTRODUCTION

High volume biomass wastes such as sewage sludge (SS) are generated in the wastewater treatment plant. SS has received considerable attention as a sustainable feedstock that can produce bio-oil and solid fuel for energy generation. But the most common treatment of SS in China is landfill. Due to the serious environmental issue and stricter legislative demands, finding proper handling for SS has drawn great attention in academia and industry. However, it is a challenge for us to recycle SS as a feedstock to generate clean energy in an efficient way because of its general characteristics: high moisture content, pathogens, heavy metals, organic compounds, high ash content, and inorganic material mixed in varying proportions.¹ Although the moisture content and toxic organic contaminants in SS are the major drawbacks for direct incineration, the abundant organics in SS can be considered as a good resource to convert into energy production via the proper treatment. One approach to producing solid fuel from SS is direct conversion to char via hydrothermal conversion (HTC).^{2,3} HTC is a wet thermochemical conversion process. The reaction of feedstock is in water at low to medium reaction

temperature (180–300 °C) and autogenerates pressure (2–10 MPa) in the absence of oxygen.^{4,5} Using HTC for biofuel production has several advantages over other types of thermochemical conversion processes, including more moderate reaction circumstances and efficient disposition of biomass without a predrying step. Furthermore, the HTC process converts solid biomass wastes into char with a high level of carbon and nutrient rich carriers in thermal processes. Therefore, it is suitable for processing aquatic biomass such as SS.^{6–8}

Currently, there are two main options for bio-oil and char production via HTC: with and without using a catalyst. The aim to mix with various catalysts is different, some aim to increase the bio-oil yield in the HTC of biomass wastes and other may enhance on generate functional materials.^{9–12} Serrano-Ruiz et al.⁹ investigated the liquid hydrocarbon fuels derived from different lignocellulosic biomass via catalytic

Received: May 2, 2018

Revised: May 22, 2018

Published: May 26, 2018

conversion. The result showed higher yields of the bio-oil and its mechanism of aqueous-phase catalytic reactions. It is noteworthy that production of biofuels from renewable sources with the catalyst is a promising route due to its ability to improve the efficiency of recycling biomass. It has been demonstrated in other research that most of the N-NH₃ and chemical oxygen demand from municipal wastewater can be removed by the hydrothermal liquefaction of *Chlorella vulgaris*. The yield of bio-oil can be gained at a maximum of 26.67% with NaOH catalyst. As an optimum example, experiments were conducted at 300 °C and remained 60 min with 2.5 wt % catalyst loading.¹⁰ Mumme et al.¹¹ studied the hydrothermal carbonization of agricultural digests for hydrochar production. Experiments were performed at HTC temperatures of 190, 230, and 270 °C. Zeolite was employed as catalyst. The major result was the higher degree of carbonization equal to 2–29 K higher reaction temperature with zeolite. Their work showed that zeolite catalysts can increase the energy and carbon recovery during the HTC of digested biomass. Moreover, the solid products showed higher surface and pore volume than the pure hydrochar.

Compared with the other catalyst, zeolites are widely used in the thermal chemical process because of their stability and efficiency, especially in the area of petroleum refining, petrochemicals, and pollution control.^{13,14} Generally, Zeolite Socony Mobil-5 (ZSM-5) may offer several advantages for a variety of thermal reactions, such as higher bio-oil yield and positive effects on the biomass pyrolysis selectivity, owing to its characteristics. These include shape selectivity, ion-exchanging properties, and large specific surface area.^{15–18} Tarach et al.¹⁹ evaluated the catalytic properties of ZSM-5 in the cracking process. The results showed the high silica hierarchical ZSM-5 can support strong stability in cracking and presented good catalytic performance. Nevertheless, the stability of ZSM-5 under relevant biomass with inorganic salts via hydrothermal conversion has been reported by Gardner et al.²⁰ The inorganic matter such as NaCl can improve the hydrolysis of the Si–O–Al bond and results in a significant effect on the condensed phase. The interaction between selectivity of glucose and ZSM-5 employing fast catalytic pyrolysis has been previously investigated by Carlson et al.²¹ It was found that the feedstock was easy to form coke because of the catalyst surface which can easily polymerize the furans group with a ratio of ZSM-5 to glucose of 19; the maximum of carbon yield was 32% and can be obtained with catalysts at 600 °C.

As indicated above, the HTC process has good performance on tackling wet biowastes such as sewage sludge under low or moderate reaction temperature. On the other hand, ZSM-5 has a positive impact during the thermal process. However, most previous effort has been devoted to the structure for the oxidation of trace organic contaminants,²² and the properties of bio-oil employ catalytic hydrothermal liquefaction and pyrolysis which are usually conducted at reaction temperatures higher than 300 °C.²³ Until recently, however, little had been performed on char production with ZSM-5 catalyst at low reaction temperature. Meanwhile, no research has been published on the application of SS with ZSM-5 catalyst in HTC, leading to a lack of understanding of chemical and structural characterization of char formation when the catalyst is introduced in the HTC. The overarching goal of this study was to give an insight into catalytic HTC that could deliver SS for transformation to an optimized char. Here, we report (i) the HTC char development in the region of moderate reaction

temperatures with ZSM-5; (ii) for comparison purposes, two types of ZSM-5 (Si/Al: 38, Si/Al: 300) introduced in the HTC; (iii) the distribution of carbons in char derived from SS which employ HTC with ZSM-5; (iv) the chemical and surface microstructure characterizations of carbon-containing group in chars; (v) a proposed reaction pathway of the carbon compound transformation during the HTC of SS with ZSM-5.

EXPERIMENTAL SECTION

Preparation of Feedstock and Catalyst. Dewatered sewage sludge was fetched from the local municipal wastewater treatment plant (Changsha, China), which contained approximately 89% moisture as feedstock. Before the experiment, the samples were dried at 105 °C overnight until the weight was stable, then, cooled in airtight containers, and ground to a fine power below 0.25 mm. In order for the comparison, hydrothermal conversion experiments employing two types of commercial ZSM-5 catalyst, with silica to alumina ratios of 38 and 300, respectively. Both SS and ZSM-5 catalyst were stored in sealed glass bottles to avoid adsorption of moisture prior to the HTC experiments.

Carbonization by Hydrothermal Conversion. All the HTC experiments were carried out in a 500 mL pressure reactor, equipped with an electromagnetic stirrer. In the HTC reactor, 20 g of SS, 10 g of ZSM-5 catalyst, and 180 g deionized water were poured into the reactor and were subsequently purged with 5 min⁻¹ N₂ flow. The reactor operates at design using temperatures of 180, 240, and 300 °C, respectively. The reaction time was held for 30, 60, and 120 min. After heating started, a temperature controller (proportional–integral–derivative (PID)) controlled the internal temperature. The magnetic stirrer was running at 120 rpm to keep the mixture well-distributed. After the reaction, the reactor was cooling down to 25 °C. Then the gas was vented into the aluminum foil sample bag. The solid and liquid product were collected and filtrated to separate them. Afterward, the char was dried in an oven at 105 °C and was subsequently ground below 0.3 mm for further analysis. In this study, each sample was named as A/B-temperature-reaction time, A/B represents the Si/Al ratio, A was 38 and B was 300. For example, sample A-240-60 refers to SS with ZSM-5 (Si/Al: 38) mixed in the reactor at 240 °C for 60 min.

SS and Char Characterization. Elemental analysis (C, H, N, and S) of the samples was carried out using an elemental analyzer, (2400 Series II, PerkinElmer, USA). Ash and volatile matter were measured with a thermogravimetric analyzer (STA 409, NETZSCH, Germany). And, the fixed carbon (FC) can be calculated by difference.⁸ The proximate analysis of the samples followed the means of standard ASTM D3174 and ASTM D3175-11. Total carbon in the aqueous phase product has been calculated by using a TOC analyzer (SHIMADZU Co., Japan). The X-ray photoemission spectra (XPS) of each SS and catalytic char have been evaluated using a K-Alpha spectrometer and an Al monochromatic X-ray anode. For the samples, the C 1s spectra by assigning binding energy at 285.0 eV. The changes in functional groups of chars were determined by a FTIR Spectrometer (8400S, USA). The sample was dried and subsequently mixed with KBr to press as disk prior to detect. One hundred scans were collected for each sample, and it was investigated within the wavelength range of 4000–400 cm⁻¹.⁴ Raman spectra were collected at constant room temperature using a 514 nm laser excitation source with a Labram-010 Raman spectrometer (Jobin Yvon, France). A microscope on a Raman spectrometer was used to focus a laser beam and collect the signal. A charge-coupled device detector was in the range from 800–1800 cm⁻¹. Every sample has been scanned 3 times to avoid useless signal.

RESULTS AND DISCUSSION

Total Carbon Balance during HTC Processes. Using a combination of the TOC and CHNS analysis, the percentage of carbon content can be calculated and is depicted in Figure 1 for the SS-derived char under various reaction temperatures. The solid residue is typically high in carbon and contains the

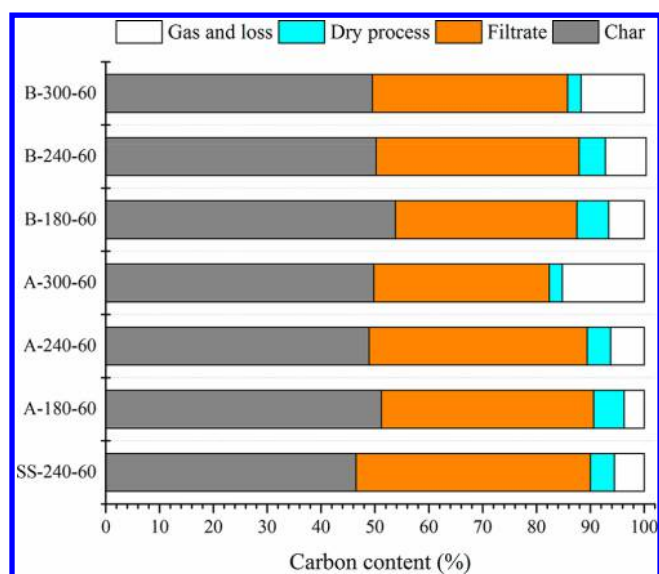


Figure 1. Carbon distribution during char production.

mineral component from the SS due to its high organic matter and ash content. Therefore, carbon in the char and filtrate contribute significantly to the carbon balance, which accounts for 82.4–90.6%. It was worth noting that the carbon content in char increased with the ZSM-5 during the HTC process. Furthermore, carbon content in the gas increased with ZSM-5 catalyst from a reaction temperature of 180 to 300 °C. This could be attributed to the decomposition of volatile matter at high reaction temperature and could result in a strong transformation of carbon into gas.²⁴ The carbon content in the dry process was lower than other samples at the reaction temperature of 300 °C, due to the low moisture content of char obtained at the high reaction temperature. For the comparison to the two types of catalyst, SS using ZSM-5 of an Si/Al ratio has generated more carbon in gas at 300 °C. Under the lower reaction temperature, the carbon content of B-180-60 in the gas phase is more than A-180-60. This suggests that the ZSM-5 catalysts (Si/Al 38) will have a positive impact on carbonization reaction under high reaction temperature, whereas the catalyst with Si/Al ratio of 300 is better to use at low temperature.

Degree of Carbonization for Chars. Carbon content is one of the most important element factors for the char. It could be affected to char structure, surface shape, and high heating

value. The impact of HTC temperature and reaction time with two type of ZSM-5 catalyst were evaluated based on the response in terms of the carbon content in the Figure 2. The trend of carbon content under various conditions can be clearly discovered. As shown in Figure 2A, higher carbon content can be obtained at the higher reaction temperature, while it was not a similar trend when prolonging holding time at lower temperature. It is possible to observe that the highest carbon content of char was produced under 60 min. And, the best reaction temperature is at 300 °C. As for the other condition, the catalyst with Si/Al ratio of 300 as shown in Figure 2B, the range of carbon content in various conditions is shorter than that of low Si/Al ratio catalyst. The appropriate conditions to produce chars with the high carbon content are a temperature of 240 °C for 60 min. This phenomenon may relate to the absorption on volatile organic compounds by the ZSM-5 with Si/Al ratio of 300. Lastly, the comparison of two types of ZSM-5 on the efficiency of carbon content suggests that ZSM-5 (Si/Al:38) was a suitable catalyst under higher reaction temperatures, and ZSM-5 (Si/Al:300) appropriately catalyzed below the reaction temperature of 240 °C.

The element data can be advantageously represented in a Van Krevelen diagram for a clear visual estimation of the coalification process of the SS derived chars with ZSM-5 catalyst via the HTC process. The upgrading areas for cellulose toward anthracite are also compared. As shown in Figure 3,

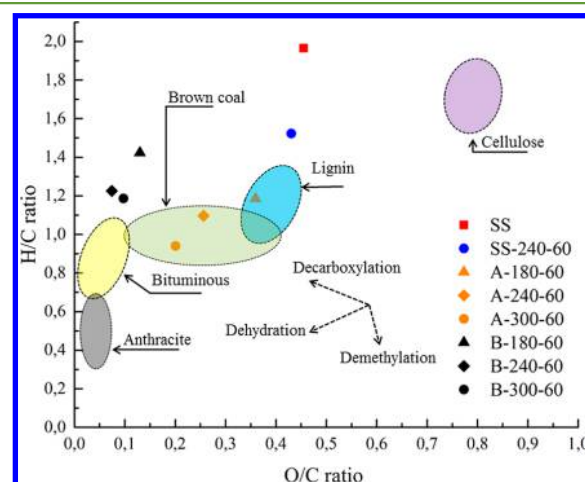


Figure 3. Van Krevelen plot of the SS and chars. Anthracite, bituminous, brown coal, lignin, and cellulose are shown for comparison.

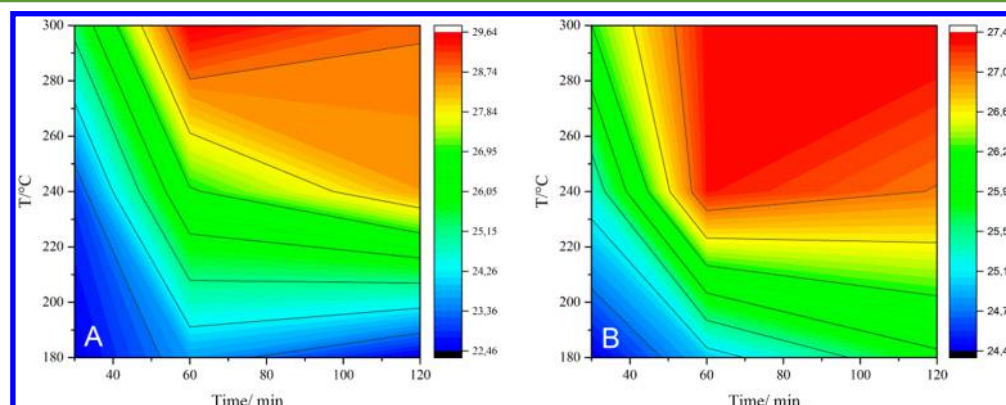


Figure 2. Carbon content in SS derived chars. (A) SS derived char with ZSM-5 (Si/Al 38). (B) SS derived char with ZSM-5 (Si/Al: 300).

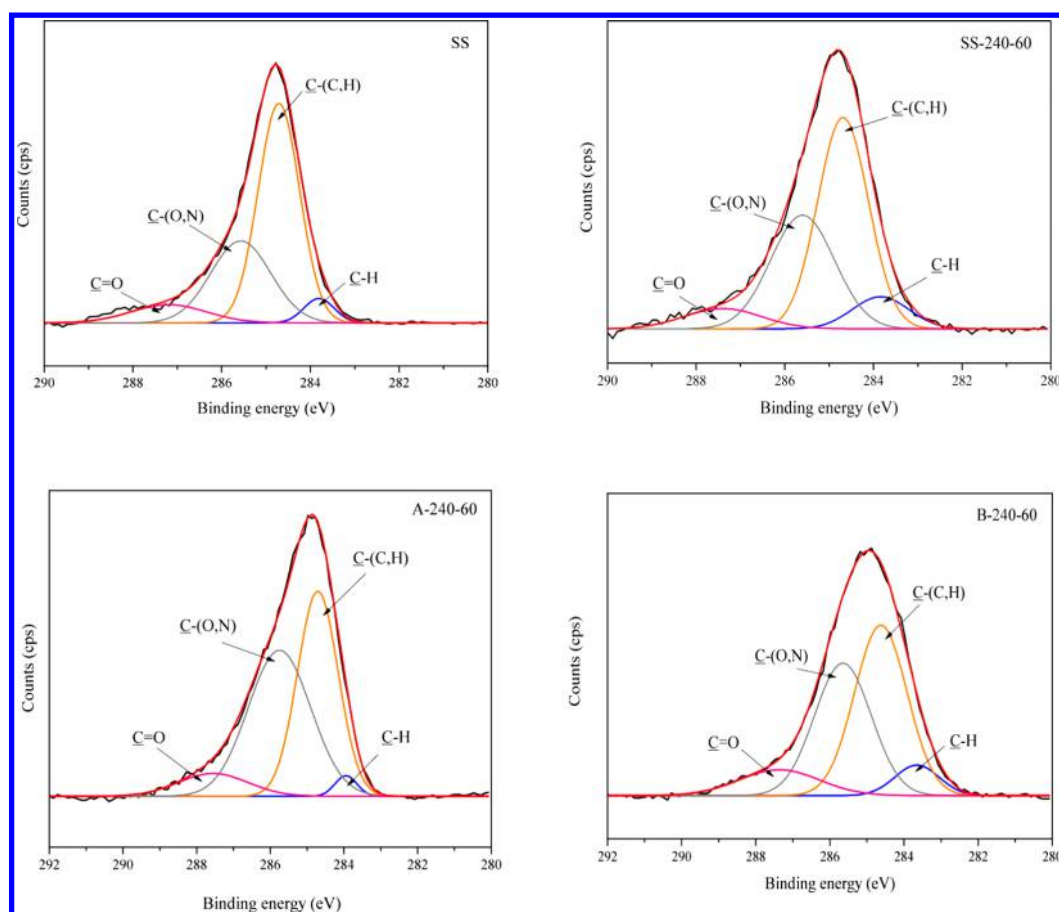


Figure 4. Dynamics of C 1s spectra of raw feedstock and char with and without two different catalysts under a reaction temperature of 240 °C for 60 min.

both H/C and O/C ratios of chars tend to reduce with the increased reaction temperature, from 1.97 and 0.46 to 1.19 and 0.36 at 180 °C reaction temperature, respectively. Moreover, the ratio of H/C showed a continuous reduction of 0.94 and O/C decreased to 0.20 when the temperature rose to 300 °C with ZSM-5 (Si/Al: 38) catalyst. On the other hand, with ZSM-5 (Si/Al: 300) assistance the H/C and O/C are within the ranges H/C 1.19–1.42 and O/C 0.07–0.13 between the reaction temperature from 180 to 300 °C. This indicated that higher reaction temperature enhanced the dehydration process of SS. Compared to the pure char, the ratio of H/C and O/C without catalyst is 1.52 and 0.43, respectively, which was even higher than the SS derived char with catalyst at 180 °C, indicating that the ZSM-5 catalyst can improve the dehydration reaction during the HTC process. Furthermore, ZSM-5 with a higher ratio of Si/Al has a significant influence on decarboxylation. However, between 240 and 300 °C, the impact of temperature and the addition of ZSM-5 were considerably lower. The similar result of the H/C and O/C trend also has been found in earlier studies on HTC biochars²⁵ and pyrolysis biochars.²⁶ Two biomass and three typical combustible materials were depicted in Figure 2 for a comparison.²⁷ The H/C and O/C of chars are higher than that of the anthracite or bituminous region, due to the high ash content of the raw feedstock. Chars with an O/C ratio in the range 0.2–0.6 are more resistant to decay, due to the graphitic sheets of it and results in a stable structure.²⁸ Hence, Chars derived from SS with ZSM-5 (Si/Al: 38) seem more stable and can be easier to store.

XPS Investigations. Figure 4 presented the XPS spectra of SS and its derived char. The C 1s XPS curve has been deconvoluted into four peaks. C–H at 283.8 eV in hydrocarbon such as cellulose, 284.5 eV for C–(C,H) also can be found in hydrocarbons, C–(O,N) at 285.7 ± 0.2 eV in amino acid, and C=O group at 287.5 ± 0.2 eV can be found in carboxylate and hemiacetals, respectively.^{8,29} The deconvolution results and the integrated areas of each functional group are represented in Table 1. The C–(C,H) functional group was the highest

Table 1. XPS Relative Integrated Areas (%) of Carbon Functionalities by Gaussian Curve Deconvolution

samples	relative integrated areas of carbon functionalities (%)			
	C–H (283.8 eV)	C–(C,H) (284.5 eV)	C–(O,N) (285.7 eV)	C=O (287.5 eV)
SS	4.55	56.39	30.59	8.47
SS-240-60	8.49	50.18	33.98	7.35
A-240-60	2.31	42.74	46.83	8.12
B-240-60	6.76	45.05	37.74	10.45

content component of the raw SS. The integrated area of C–(C,H) accounted for 56.39%, followed by 30.59% of C–(O,N), and 8.47% of C=O. C–H was relative the lowest which accounted for 4.55%. After the HTC process, two C 1s spectra shown a significant distinction according to the impact of the catalyst. The first is the char with ZSM-5 (Si/Al 38) assistance. The integrated area of C–(O,N) showed a significant enhancement, whereas the C–(C,H) and C–H peaks were

distinctly reduced under the HTC process. The integrated area of the last small peak of C=O (287.5 eV) remained stable under the HTC process. Aromatic C-(C,H) and C-H groups reduced after the reaction, revealing that those two aromatic groups depolymerized at about 240 °C. Besides, C-(O,N) accounts for a high content of 46.83% and became the predominant carbon functionality in char, which may be related to the decomposition of hydrocarbon mainly originated from carbohydrates and lipids. Meanwhile, ZSM-5 (Si/Al: 38) catalyst could assist in generating some multifunctional organic groups during the reaction.³⁰ Another distinction is the char derived from SS with ZSM-5 (Si/Al: 300). The integrated area of C-(C,H) reduced to 45.05%, but the other groups C-H, C-(O,N), and C=O increased to 6.76%, 37.74%, and 10.45% respectively, resulting from the recombination of C-(C,H) at high reaction temperature. On the other hand, the presence of hydroxyl groups can be found in the low concentration of ethers and phenols. Above all, to compare with SS and its derived char, the main effect of ZSM-5 on the C-containing group are the decomposition of C-(C,H) under a moderate condition and the formation of C-(O,N) structure.

FTIR Analysis of SS and Char. Figure 5 presented the FTIR spectra of the feedstock and char. The transmittance

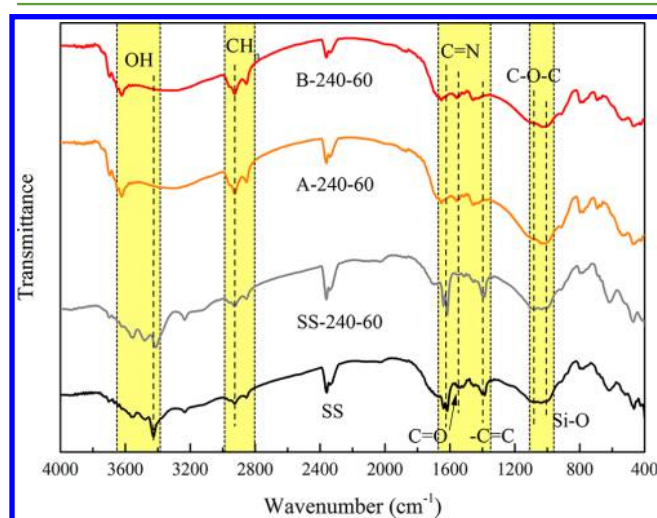


Figure 5. FTIR spectra of SS and its HTC char with and without ZSM-5 catalyst.

peaks which provided their chemical composition was compared according to the basis of previous researches. In general, the main identification peak can be separated by four regions. And the peak at about 2300–2400 cm^{-1} was related to the uncontrollable CO_2 from the measurement atmosphere. Moreover, the characteristic of functional groups in chars was similar even added with two type of ZSM-5 catalyst. But the organic functional groups have an obvious change in the char spectra reduced as a result of HTC, especially after use ZSM-5 catalyst. The following details were drawn according to the peaks:^{31–34}

- (i) The broad band at around 3300–3500 cm^{-1} is (–OH) which results from the free hydroxyl bonded or carboxyl functional group. After the HTC process without ZSM-5 catalyst, the peak of the char shown a slightly less intense. However, the peak intensity decreased rapidly and acquired a rounded tip for the chars derived from SS with ZSM-5 catalyst, indicating that ZSM-5 catalyst can

improve the dehydration during the HTC. It is related to the conversion of water, alcohol, and phenol.³⁵

- (ii) The broad band from 2800 to 3000 cm^{-1} was attributed to the $-\text{CH}_n$ functional group. Furthermore, the weak peak at 2920 and 2850 cm^{-1} are $-\text{C}-\text{H}$ groups from the fats component of SS.³⁶ The peak shows no significant change between SS and char. However, after the ZSM-5 catalyst is added, the bond of $-\text{CH}_n$ exhibited a significant increase after HTC, which could be explained by the formation of several long aliphatic chains following HTC.³⁷
- (iii) Three identical peaks can be found from 1350 to 1650 cm^{-1} . The first peak at 1645 cm^{-1} was assigned to the C=N functional group which resulting from the amides. The peak intensity decreased rapidly at the char sample of A-240-60 and B-240-60, suggesting a strong hydrolyzation of amides occurred when ZSM-5 catalyst was added during the HTC. Meanwhile, the second peak at 1540 cm^{-1} is caused by the stretching of $-\text{C}=\text{O}$ in the carboxylic groups. The peak seems to have disappeared after HTC, which could be explained by a decrease in the decarboxylation reaction. And the last peak at 1455 cm^{-1} is a $-\text{C}=\text{C}$ group which can be found in the aromatic ring carbons. The $-\text{C}=\text{C}$ functional group slightly enhanced after the HTC process, indicating more heteroaromatic structures were formed by the aromatization reaction.³⁸
- (iv) The strong band at 1100–950 cm^{-1} in all the samples was caused by C–O–C stretching vibration which can be found in aliphatic ether and esters. The C–O–C group in char slightly reduced because the alcohol component dehydrated during the reaction.³⁹ Meanwhile, another intensity peak at 1000 cm^{-1} in char samples corresponds to Si–O stretching of clay minerals, and it indicated the presence of silicate impurities in the feedstock.⁴⁰ Si is noted in the presence as ash content in the SS-derived char.

Raman Analysis of SS and Char. Raman spectrum was also used to an in-depth study on chemical composition and carbon-containing structure of SS and SS-derived char. Figure 6 shows the result in the range from 1000 to 1800 cm^{-1} . For the spectra studied, a fitting analysis has been conducted with eight Gaussian bands. Table 2 defines the typical structures used in Figure 6 along with the best-fit position. After the HTC process, band V_L and S_L in SS significantly decreased, indicating that the content of small polyaromatic groups that grafted with amorphous carbon structures reduced sharply and the aromatic structures had been formed in char. Figure 7 present the D/G and $D/(G_R + V_R + V_L)$ band area ratios of SS and char samples. The value of I_D/I_G could be used to measure of the graphitic degree of carbons. And the aromatic ring structure breathing mode was confirmed by the value of $G_R + V_R + V_L$; therefore, the $I_D/I_{(G_R+V_R+V_L)}$ is the ratio between polyaromatic ring and aromatic ring. The I_D/I_G ratio increases after the HTC process. Especially for the sample which added with ZSM-5 (Si/Al: 300), the I_D/I_G ratio obtained the peak, indicating that the graphitic degree of carbons shows a strong enhancement. This effect was caused by the dehydrogenation reaction and the generation of polyaromatic ring structure after the HTC process.⁴¹ The value of $I_D/I_{(G_R+V_R+V_L)}$ steadily increases as the raw SS added ZSM-5 catalyst. The ratio of chars derived from SS added with ZSM-5 (Si/Al 300) was still the highest, which

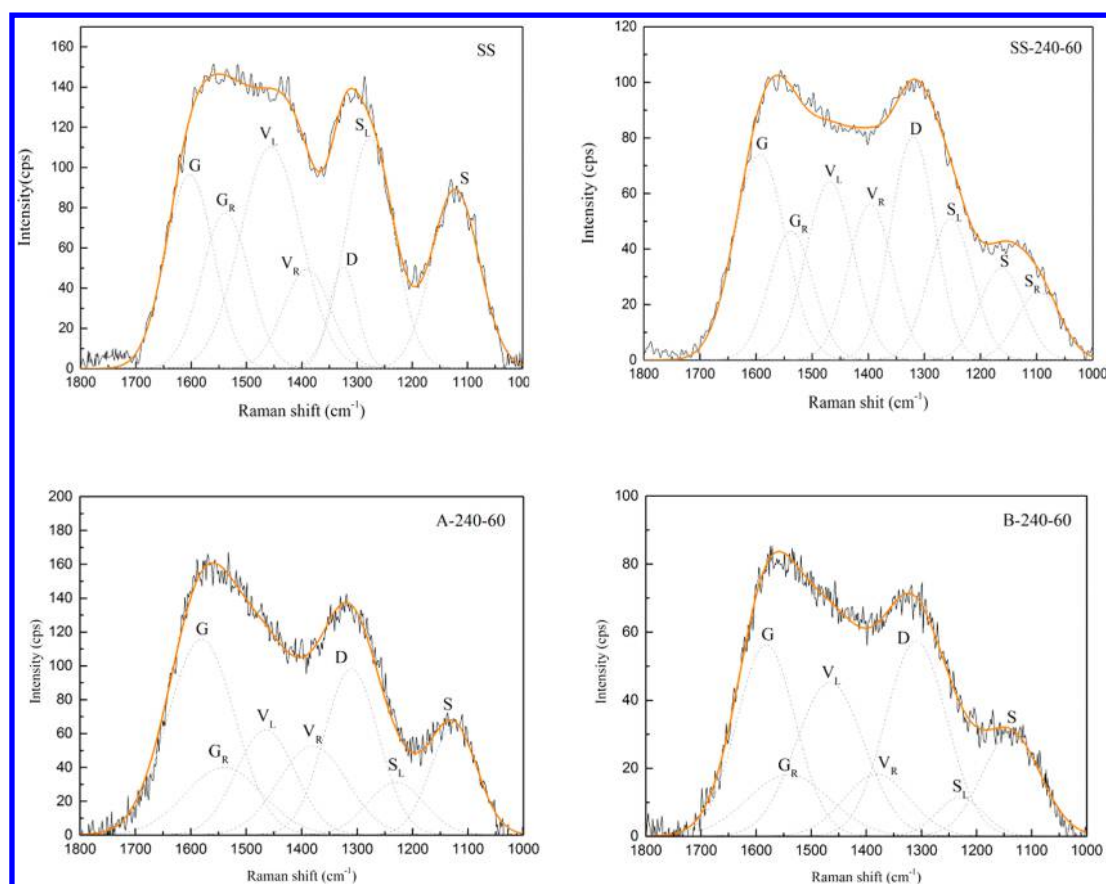


Figure 6. Raman spectra deconvolution with fitting results using eight Gaussian bands of the SS and char obtained under 240 °C.

Table 2. Char Composition Features as Deduced from Fitting the Raman Assignments for Disordered Carbon^{42,43}

band name	position (cm ⁻¹)	attribution
G	1580	presence of graphitic crystallites; well-structured aromatic rings
G _R	1540	coexistence of well-structured and amorphous carbon structures
V _L	1465	structural defects of aromatic clusters; amorphous carbon structures
V _R	1380	not well-structured aromatics
D	1310	amorphous or disordered graphite
S _L	1230	C–O bond fomation; para-aromatics
S	1180–1100	C–O–C bond fomation; C–C bond fomation
S _R	1100–1050	C–H bond on aromatics

reveals that there are still a number of small aromatic rings with amorphous structure in the char due to the fact that aromatic compounds have still not fully polymerized under moderate reaction temperatures even with ZSM-5 assistance.⁴² As the ZSM-5 catalyst was added during HTC process, a clearly observed increase of polymerizing carbon groups in char is consistent with those in the earlier literature.^{43,44}

Conversions of Carbon-Containing Groups in Char.

According to the previous research, the most abundant organic matter in SS is the cellulose, proteins, and lipids, which can be conformed through XPS analysis. ZSM-5 catalyst could cause SS to heat uniformly by its special physical shape and can promote the reaction process which has been proved in the early analysis. A possible reaction pathway of carbon compound transformation during the HTC process is shown in Figure 8.

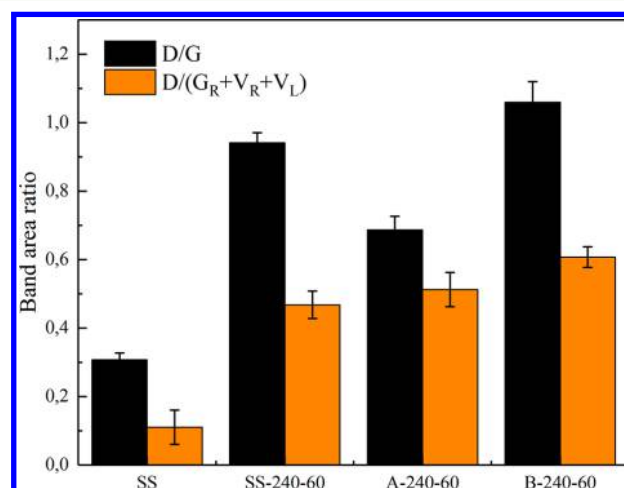


Figure 7. Band area ratios between SS and SS-derived chars.

The transformation of carbon-containing groups in the HTC process has been thoroughly reviewed by several authors.^{45–47} Under hydrothermal conditions, cellulose undergoes hydrolysis to form glucose and fructose and then it can convert to furans by dehydration (route a). On the other hand, some different short intermediate groups such as C=O and C=C were formed by the C–C splitting. These functional groups caused gas to be generated including CO₂, CO, and CH₄. Moreover, these groups could convert to phenols under a certain condition. Proteins are major biomass components, which consist of one or several peptide chains. The peptide bond is the key to link amino acids together. When it was broken, the

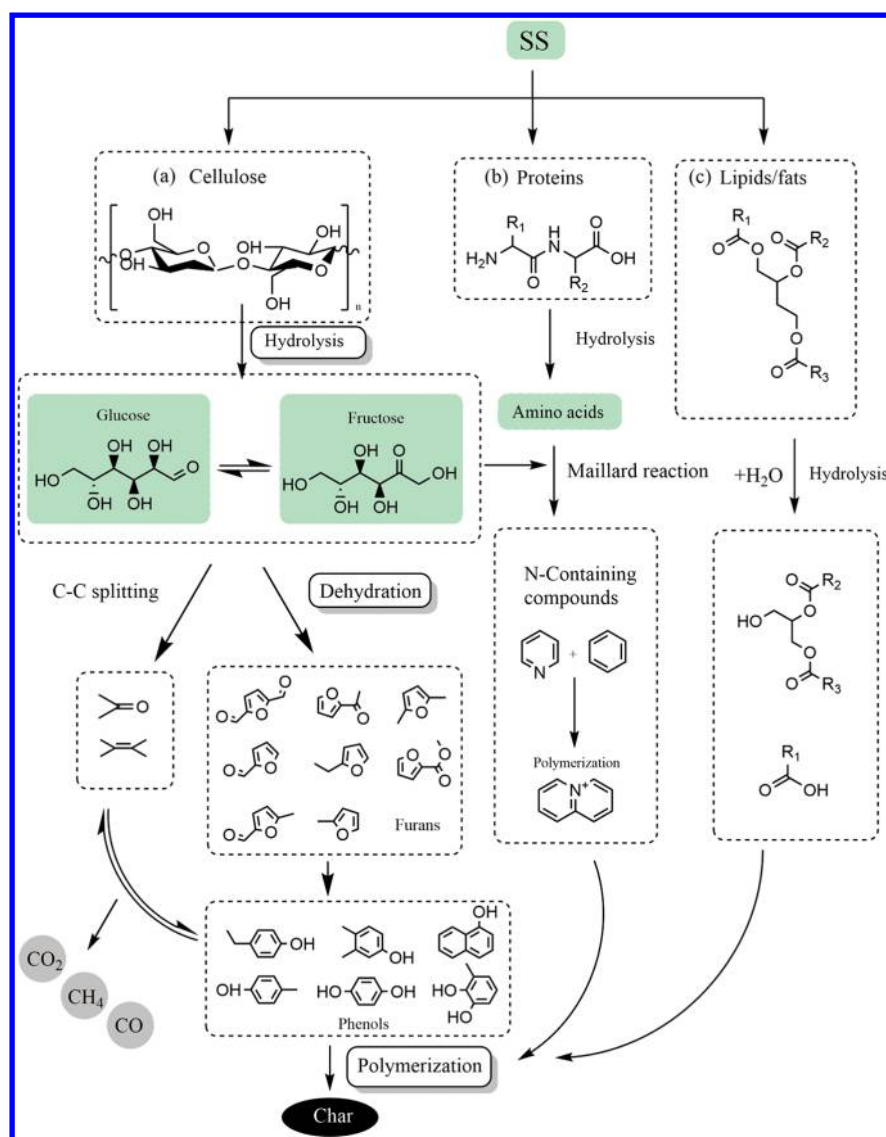


Figure 8. Simplified scheme of the predominate carbon compounds in SS-derived char via HTC process with catalyst.

protein began to hydrolyze to labile amides during the HTC process (route b). Those amino acids undergo similar decarboxylation. Furthermore, the N-containing compounds such as pyridines and pyrroles can be formed by the amino acids and sugars via the Maillard reaction. Those mixture compounds are common components in char and liquid produced by the HTC process of SS.⁴⁸ This also can be proven by the reduction of the C=N group which has been found in the FTIR analysis. Lipids and fats could be soluble in liquid under moderate reaction temperature, which is caused by the low dielectric constant of water, and greater miscibility could occur.⁴⁹ The hydrolysis of lipids/fats occurred when the ester bonds were broken. The major decomposition mechanism was decarboxylation which can be found in the Van Krevelen plot. Moreover, this decomposition would cause C=O and C-(C,H) groups to decrease, which has been proven by the XPS analysis results. It is reasonable to assume this pathway of carbon transformation in char during the HTC process, further emphasizing that the investigation of advanced catalysts has a positive impact on improving HTC technology.

Implications for Future Research. In the present work, the effect of ZSM-5 catalyst on the carbon-containing

compounds transformation through HTC under various conditions was investigated. The distribution of carbon content, the degree of carbonization, the chemical composition of carbon compounds, and carbon structure were measured to analyze the trend of carbon contents in the char production via the HTC process. A simplified reaction pathway of carbon transformation has been proposed. This work advances the understanding of SS-derived char using the HTC process with ZSM-5 and may provide opportunities for advancing the current understanding of the mechanism of char production. However, a large-scale HTC process using ZSM-5 catalyst will face several issues. The whole system should be stable when the temperature increase and the feedstock should be tackled in a continuous reactor. Furthermore, the mass balance and energy consumption of the process should be taken into account, but it is complicated to calculate the accuracy number of energy input and output, especially in a pilot scale test. On the other hand, the inorganic composition in sewage sludge could significantly influence the shape, yield, and structure of the char because some of them will transform their morphology during the thermal process. Anyway, sewage sludge is just one of the wet biomass wastes. To find out which part of the composition in

biomass wastes can be converted into biofuel using the HTC process with ZSM-5, several model compounds could be investigated in the future. Finally, to combine with HTC process and ZSM-5 catalyst and then put it into practical use, some studies should be considered as follows: (a) test of biomass wastes on a pilot scale HTC process equipped with a continuous reactor, (b) measurement and calculation of the energy and mass balance, (c) investigation of inorganic composition effect on the efficiency of the HTC process with ZSM-5 catalyst, and (d) exploration of the HTC process mechanism using model compounds.

AUTHOR INFORMATION

Corresponding Authors

*Tel.: +86 731 8882 2829. Fax: +86 731 8882 2829. E-mail

Address: ybzhai@hnu.edu.cn (Yunbo Zhai)

*E-mail: zhuyun@hnu.edu.cn (Yun Zhu).

ORCID

Yunbo Zhai: 0000-0001-8164-0613

Caiting Li: 0000-0002-7046-2214

Guangming Zeng: 0000-0002-4230-7647

Notes

The authors declare no competing financial interest.

ACKNOWLEDGMENTS

This research was financially supported by a project of the National Natural Science Foundation of China (No. 51679083), the Interdisciplinary Research Funds for Hunan University (2015JCA03), a scientific and technological project of Changsha City (KQ1602029), the financial support from the program of China Scholarships Council (No. 201706130088), a project of Shenzhen Science and Technology Funds (JCYJ20160530193913646), and the State Key Laboratory of pollution control and treatment of petroleum and petrochemical industry (PPC2017003).

REFERENCES

- Bagreev, A.; Badosz, T. J.; Locke, D. C. *Carbon* **2001**, *39* (13), 1971–1979.
- Zhao, P.; Shen, Y.; Ge, S.; Chen, Z.; Yoshikawa, K. *Appl. Energy* **2014**, *131*, 345–367.
- Zhai, Y.; Liu, X.; Zhu, Y.; Peng, C.; Wang, T.; Zhu, L.; Li, C.; Zeng, G. *Bioresour. Technol.* **2016**, *218*, 183–188.
- Peng, C.; Zhai, Y.; Zhu, Y.; Xu, B.; Wang, T.; Li, C.; Zeng, G. *Fuel* **2016**, *176*, 110–118.
- Wang, T.; Zhai, Y.; Zhu, Y.; Peng, C.; Xu, B.; Wang, T.; Li, C.; Zeng, G. *Bioresour. Technol.* **2018**, *247*, 182–189.
- Zhai, Y.; Chen, H.; Xu, B.; Xiang, B.; Chen, Z.; Li, C.; Zeng, G. *Bioresour. Technol.* **2014**, *159*, 72–79.
- He, C.; Giannis, A.; Wang, J.-Y. *Appl. Energy* **2013**, *111*, 257–266.
- Peng, C.; Zhai, Y.; Zhu, Y.; Wang, T.; Xu, B.; Wang, T.; Li, C.; Zeng, G. *J. Cleaner Prod.* **2017**, *166*, 114–123.
- Serrano-Ruiz, J. C.; Dumesic, J. A. *Energy Environ. Sci.* **2011**, *4* (1), 83–99.
- Arun, J.; Shreekanth, S. J.; Sahana, R.; Raghavi, M. S.; Gopinath, K. P.; Gnanaprakash, D. *Bioresour. Technol.* **2017**, *244*, 963–968.
- Mumme, J.; Titirici, M.-M.; Pfeiffer, A.; Lüder, U.; Reza, M. T.; Mašek, O. *ACS Sustainable Chem. Eng.* **2015**, *3* (11), 2967–2974.
- Chen, H.; Zhai, Y.; Xu, B.; Xiang, B.; Zhu, L.; Li, P.; Liu, X.; Li, C.; Zeng, G. *Energy Convers. Manage.* **2015**, *89*, 955–962.
- Rahimi, N.; Karimzadeh, R. *Appl. Catal., A* **2011**, *398* (1–2), 1–17.
- Corma, A.; Rey, F.; Rius, J.; Sabater, M. J.; Valencia, S. *Nature* **2004**, *431* (7006), 287–290.
- Song, Z.; Takahashi, A.; Nakamura, I.; Fujitani, T. *Appl. Catal., A* **2010**, *384* (1–2), 201–205.
- Paillaud, J.-L.; Harbuzaru, B.; Patarin, J.; Bats, N. *Science (Washington, DC, U. S.)* **2004**, *304* (5673), 990–992.
- Jung, J. S.; Park, J. W.; Seo, G. *Appl. Catal., A* **2005**, *288* (1–2), 149–157.
- Corma, A.; Díaz-Cabañas, M. J.; Martínez-Triguero, J.; Rey, F.; Rius, J. *Nature* **2002**, *418* (6897), 514–517.
- Tarach, K. A.; Martínez-Triguero, J.; Rey, F.; Góra-Marek, K. J. *Catal.* **2016**, *339*, 256–269.
- Gardner, D. W.; Huo, J.; Hoff, T. C.; Johnson, R. L.; Shanks, B. H.; Tessonnier, J.-P. *ACS Catal.* **2015**, *5* (7), 4418–4422.
- Carlson, T. R.; Jae, J.; Lin, Y.-C.; Tompsett, G. A.; Huber, G. W. *J. Catal.* **2010**, *270* (1), 110–124.
- Xiao, R.; Ye, T.; Wei, Z.; Luo, S.; Yang, Z.; Spinney, R. *Environ. Sci. Technol.* **2015**, *49* (22), 13394–13402.
- Du, S.; Valla, J. A.; Bollas, G. M. *Green Chem.* **2013**, *15* (11), 3214.
- Magdziarz, A.; Werle, S. *Waste Manage. (Oxford, U. K.)* **2014**, *34* (1), 174–179.
- Reza, M. T.; Rottler, E.; Herklotz, L.; Wirth, B. *Bioresour. Technol.* **2015**, *182*, 336–344.
- van der Stelt, M. J. C.; Gerhauser, H.; Kiel, J. H. A.; Ptasinski, K. J. *Biomass Bioenergy* **2011**, DOI: 10.1016/j.biombioe.2011.06.023.
- Park, S.-W.; Jang, C.-H. *Waste Manage. (Oxford, U. K.)* **2011**, *31* (3), 523–529.
- Licursi, D.; Antonetti, C.; Fulignati, S.; Vitolo, S.; Puccini, M.; Ribecchini, E.; Bernazzani, L.; Raspolli Galletti, A. M. *Bioresour. Technol.* **2017**, *244*, 880–888.
- He, C.; Zhao, J.; Yang, Y.; Wang, J.-Y. *Bioresour. Technol.* **2016**, *211*, 486–493.
- Huang, Z.; Lu, Q.; Wang, J.; Chen, X.; Mao, X.; He, Z. *PLoS One* **2017**, *12* (8), e0183617.
- Francioso, O.; Rodriguez-Estrada, M. T.; Montecchio, D.; Salomoni, C.; Caputo, A.; Palenzona, D. *J. Hazard. Mater.* **2010**, *175* (1–3), 740–746.
- Liu, Z.; Zhang, F.-S.; Wu, J. *Fuel* **2010**, *89* (2), 510–514.
- Jin, Z.; Chang, F.; Meng, F.; Wang, C.; Meng, Y.; Liu, X.; Wu, J.; Zuo, J.; Wang, K. *Chemosphere* **2017**, *184*, 1043–1053.
- Domínguez, A.; Menéndez, J. A.; Inguanzo, M.; Pis, J. J. *Bioresour. Technol.* **2006**, *97* (10), 1185–1193.
- Wei, L.; Liang, S.; Guho, N. M.; Hanson, A. J.; Smith, M. W.; Garcia-Perez, M.; McDonald, A. G. *J. Anal. Appl. Pyrolysis* **2015**, *115*, 268–278.
- Grube, M.; Lin, J. G.; Lee, P. H.; Kokorevicha, S. *Geoderma* **2006**, *130* (3–4), 324–333.
- Kruse, A.; Gawlik, A. *Ind. Eng. Chem. Res.* **2003**, *42* (2), 267–279.
- Novak, J. M.; Busscher, W. J.; Watts, D. W.; Laird, D. A.; Ahmedna, M. A.; Niandou, M. A. S. *Geoderma* **2010**, *154* (3–4), 281–288.
- Areeprasert, C.; Zhao, P.; Ma, D.; Shen, Y.; Yoshikawa, K. *Energy Fuels* **2014**, *28* (2), 1198–1206.
- Zhang, J.; Lü, F.; Zhang, H.; Shao, L.; Chen, D.; He, P. *Sci. Rep.* **2015**, *5*, 9406.
- LI, X.; HAYASHI, J.; LI, C. *Fuel* **2006**, *85* (12–13), 1700–1707.
- Asadullah, M.; Zhang, S.; Min, Z.; Yimsiri, P.; Li, C.-Z. *Bioresour. Technol.* **2010**, *101* (20), 7935–7943.
- SHENG, C. *Fuel* **2007**, *86* (15), 2316–2324.
- Timko, M. T.; Maag, A. R.; Venegas, J. M.; McKeogh, B.; Yang, Z.; Tompsett, G. A.; Escapa, S.; Toto, J.; Heckley, E.; Greenaway, F. T. *RSC Adv.* **2016**, *6* (15), 12021–12031.
- Op de Beeck, B.; Dusselier, M.; Geboers, J.; Holsbeek, J.; Morré, E.; Oswald, S.; Giebler, L.; Sels, B. F. *Energy Environ. Sci.* **2015**, *8* (1), 230–240.
- Johnson, M. C.; Tester, J. W. *Ind. Eng. Chem. Res.* **2013**, *52* (32), 10988–10995.

- (47) Toor, S. S.; Rosendahl, L.; Rudolf, A. *Energy* **2011**, *36* (5), 2328–2342.
- (48) Kruse, A.; Maniam, P.; Spieler, F. *Ind. Eng. Chem. Res.* **2007**, *46* (1), 87–96.
- (49) Peterson, A. A.; Vogel, F.; Lachance, R. P.; Fröling, M.; Antal, J. M., Jr.; Tester, J. W. *Energy Environ. Sci.* **2008**, *1* (1), 32.